Interband Faraday rotation in diluted magnetic semiconductors: $Zn_{1-x}Mn_xTe$ and $Cd_{1-x}Mn_xTe$

D. U. Bartholomew, J. K. Furdyna, and A. K. Ramdas
Department of Physics, Purdue University, West Lafayette, Indiana 47907
(Received 9 June 1986)

Faraday rotation as a function of Mn^{2+} concentration (x), temperature, and magnetic field is measured in the zinc-blende diluted magnetic semiconductors $Zn_{1-x}Mn_xTe$ and $Cd_{1-x}Mn_xTe$. The effects of the large exchange interaction between d electrons of Mn^{2+} and the Γ_6 conduction-band electrons as well as the Γ_8 valence-band electrons are strikingly manifested in the interband Faraday effect leading to very large rotations. For large x, the effects of Mn^{2+}-Mn^{2+} antiferromagnetic exchange interaction are observed in the temperature dependence of the Faraday rotation.

I. INTRODUCTION

Diluted magnetic semiconductors (DMS's) are alloys in which atoms of a group-II element of a II-VI compound semiconductor are randomly replaced by magnetic atoms. Such alloys exhibit many striking properties.[1,2] For example, the presence of the magnetic ion Mn^{2+} in a DMS such as $Cd_{1-x}Mn_xTe$ (CMT) or $Zn_{1-x}Mn_xTe$ (ZMT) results in a Mn^{2+}-Mn^{2+} antiferromagnetic interaction which eventually (at high magnanese concentration x and low temperature T) leads to the formation of a magnetically ordered phase.[3] In addition, spin-spin exchange interaction also occurs between the d electrons of the Mn^{2+} ions and the s-like conduction-band and and the p-like valence-band electrons (sp-d exchange interaction), which, in turn, profoundly affects all physical phenomena dependent on the Zeeman splitting of the band extrema. The spectacular enhancement of the Faraday rotation[4] exhibited by DMS (the so called *giant Faraday rotation)* is a consequence of such Mn^{2+}-band electron exchange interaction. Faraday rotation has been reported for CMT (Ref. 4) for a series of manganese concentrations and temperatures, and for ZMT (Ref. 5) for $x=0.10$ and $T=77$ K. As will be discussed later, the magnitude of this rotation depends on the sp-d exchange coupling for the given alloy system, as well as on its magnetization.

The Faraday rotation in DMS alloys is in general very large, with a sign *opposite* to that in nonmagnetic II-VI compounds.[6] In order to observe how this sign reversal develops, we have studied the Faraday effect in CMT and ZMT in the limit of very small manganese concentrations. We have also investigated the Faraday effect in $Zn_{1-x}Mn_xTe$ over a wide range of x at room temperature and in $Cd_{1-x}Mn_xTe$ for a series of x values as a function of temperature spanning the paramagnetic and the magnetically ordered phases. In the present paper we report and discuss the results of these studies.

II. EXPERIMENT

The samples used in our investigations were single crystals of CMT and ZMT grown by the vertical Bridgman method. They were optically polished, using successively finer abrasives and polishing compounds, the final polish being accomplished with 0.05-μm alumina powder. The samples had typical dimensions of $5\times5\times3$ mm. The manganese concentration was determined from electron-probe microanalysis and/or density measurements. For $x<0.05$ such measurements are not sensitive enough and the nominal values are used to characterize the samples.

For room and liquid-nitrogen temperatures, Faraday rotation was measured by placing the sample in a magnetic field of an electromagnet,[7] and between two polaroid sheets set at 45° with respect to each other.[8] Using this apparatus, rotations as small as 0.1° could be easily determined. Faraday rotation as a function of photon energy was measured using a single-pass monochromator having a bandwidth of 10 meV, with a tungsten-halogen lamp serving as the light source. The transmitted light was detected with a silicon p-i-n diode. For temperatures below 77 K, the samples were placed in a variable-temperature optical cryostat equipped with a superconducting coil.[9] The sample was again placed between two polarizers, and the light transmitted by the combination was spectrally analyzed with a double monochromator,[10] an incandescent lamp serving as the light source. A typical transmission curve is shown in Fig. 1 observed for $Cd_{0.77}Mn_{0.23}Te$ at $T=5$ K and a magnetic field H of 5 kG. Each successive peak in the spectrum represents an additional Faraday rotation of 180°. The absolute Faraday rotation as a function of frequency is determined by monitoring the transmission at several fixed photon energies as the magnetic field is swept. By setting the polarizer and the analyzer at angles other than 45° with respect to each other, the entire Faraday-rotation dispersion can be determined. This technique works very well for DMS's where the slope of this dispersion does not change sign and where the rotations are large (for example, at low temperatures).

III. THEORY

In order to discuss Faraday rotation, we consider monochromatic radiation of angular frequency ω traveling in a cubic crystal along an external magnetic field $\mathbf{H}\|\hat{\mathbf{z}}$, where

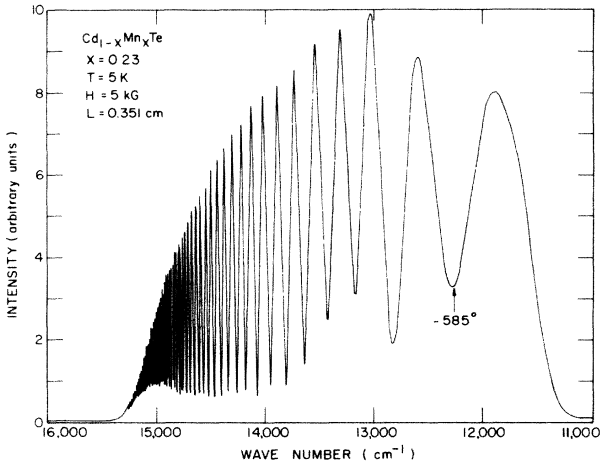

FIG. 1. Transmission spectrum through $Cd_{1-x}Mn_xTe$, $x=0.23$, in the Faraday geometry at $T=5$ K and $H=5$ kG displaying giant Faraday rotations several orders of magnitude larger than those seen in CdTe. The intensity cutoff at low photon energies is due to the photomultiplier-tube response, whereas the cutoff at high energies is due to the absorption edge of the sample. The minima of the transmission oscillations are not zero as a result of increasing Faraday ellipticity near the absorption edge.

$\hat{\mathbf{x}}$, $\hat{\mathbf{y}}$, and $\hat{\mathbf{z}}$ define a right-handed coordinate system (see Fig. 2). In this configuration (the Faraday geometry), light propagating parallel to **H** is described by the two different indices of refraction corresponding to the two circular polarizations of positive and negative helicity, defined by the two counterrotating unit vectors

$$\hat{\sigma}_{\pm}=\frac{1}{\sqrt{2}}(\hat{\mathbf{x}}\pm i\hat{\mathbf{y}})e^{-i\omega t} .$$

As a result, linearly polarized light traveling through the sample in this geometry will experience a rotation of the plane of polarization. This phenomenon is called Faraday

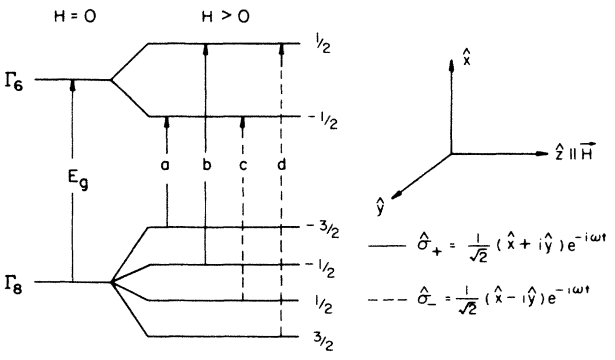

FIG. 2. To the left, schematic illustration of the transitions between the spin-split valence-band maxima and conduction-band minima allowed in the Faraday geometry. To the right, coordinate system defining the Faraday geometry and the definition of the two circular polarizations of light.

rotation. The polarization of the transmitted light may also show some degree of ellipticity if there is significant circular dichroism induced by the magnetic field.[11] By convention, rotations which are counterclockwise when viewed against the light propagating along the direction of the magnetic field are defined as positive.[6] In discussing Faraday rotation, it is convenient to introduce a *specific rotation,* in units of degrees per unit magnetic field (G) per unit length (cm), referred to as the Verdet constant V. In general, V is a function of photon energy, temperature, and, in the case of DMS alloys, the magnetic characteristics of the crystal.

Faraday rotation Θ_F is given by the well-known expression

$$\Theta_F=\frac{El}{2\hbar c}(n_- - n_+) , \tag{1}$$

where E is the photon energy, l the distance in the medium traversed by the light, c the speed of light in vacuum, and $n_{\pm}$ the indices of refraction for the two circular polarizations $\hat{\sigma}_{\pm}$. Before discussing the microscopic origin of the circular birefringence (i.e., the fact that $n_+ \neq n_-$), which clearly has to be sought in electronic transitions in the presence of an external magnetic field, we first consider the index of refraction for $H=0$. In the absence of the field, the dispersion of the refractive index has the form

$$n^2-1 \propto \sum_{i,j}\frac{f_{ij}}{E_{ij}^2-E^2} , \tag{2}$$

where E_{ij} is the transition energy (E_j-E_i) between the energy levels i and j, and f_{ij} is the oscillator strength. The electronic transitions of significance in a wide-band-gap DMS are (1) interband and excitonic transitions, (2) intraband transitions, (3) transitions associated with the internal levels of Mn^{2+}, and (4) those associated with impurities and lattice defects. All these transitions will, in principle, contribute to circular birefringence—and thus to the Faraday effect—if they exhibit a Zeeman splitting in the presence of the applied field H.

For frequencies close to a given electronic transition E_{ij}, the refractive index given by Eq. (2) will be dominated by the term corresponding to that transition. The difference between n_+ and n_- can then be related to the energy difference ΔE_{ij} between transitions observed in $\hat{\sigma}_+$ and $\hat{\sigma}_-$ polarizations. By Taylor expansion one can then show that, to first order in ΔE_{ij},

$$(n_- - n_+)=\frac{\partial n}{\partial E}\Delta E_{ij} . \tag{3}$$

Thus

$$\Theta_F=\frac{El}{2\hbar c}\frac{\partial n}{\partial E}\Delta E_{ij} . \tag{4}$$

The theory of the interband Faraday effect in semiconductors has been developed by Boswarva *et al.*[12] and Roth.[13] These theories have been applied to many systems, including II-VI compound semiconductors.[6,14] For DMS alloys, in the spectral range investigated, the exciton transitions appear to play a dominant role in determining the Faraday effect. One can thus specialize our discussion

to a single oscillator of energy E_0 in Eq. (2). The refractive index can then be expressed by

$$n^2=n_0^2+F_0(E_0^2-E^2)^{-1} ,$$

where F_0 is a constant involving, among others, the oscillator strength of the excitonic transition, and n_0 represents all contributions to n other than that associated with E_0. Using this form of n in Eq. (3), we obtain

$$\Theta_F=\frac{F_0 l}{2\hbar c}\frac{1}{n}\frac{E^2}{(E_0^2-E^2)^2}\Delta E_0 , \tag{5}$$

where n is the refractive index in the absence of a magnetic field. For E close to E_0, we may assume that $n^2=F_0(E_0^2-E^2)^{-1}$. Hence,

$$\Theta_F=\left[\frac{\sqrt{F_0}l}{2\hbar c}\Delta E_0\right]\frac{1}{E_0}\frac{y^2}{(1-y^2)^{3/2}} , \tag{6a}$$

i.e.,

$$V(E)=\frac{D}{E_0}\frac{y^2}{(1-y^2)^{3/2}} , \tag{6b}$$

where $y=E/E_0$ and

$$D=\frac{\sqrt{F_0}}{2\hbar c}\frac{\partial\Delta E_0}{\partial H} .$$

Shallow impurity and intraband transitions are far from E_0, and are therefore ignored in Eq. (6a). The transitions associated with the internal levels of Mn^{2+} are not seen to split in a magnetic field[15] and are also not likely to contribute to the Faraday-rotation dispersion.

As we mentioned in the Introduction, the very large size of the Faraday effect in DMS's arises from the fact that in these materials the *sp-d* exchange interaction leads to an enhanced spin splitting of the electronic energy bands or, equivalently, to large effective g factors. This splitting of the bands is described as follows. The Γ_6 conduction-band minimum splits into two levels given by $E_g\pm 3A$, and the Γ_8 valence-band maximum into four levels given by $\pm B$ and $\pm 3B$, as shown schematically in Fig. 2. Here the zero for the energy scale is defined by the valence-band maximum at $H=0$; E_g is the zero-field energy gap at $k=0$,

$$A=\tfrac{1}{6}\alpha\frac{M}{g_{\mathrm{Mn}}\mu_B}$$

and

$$B=\tfrac{1}{6}\beta\frac{M}{g_{\mathrm{Mn}}\mu_B} ,$$

α and β are the exchange integrals for the conduction- and valence-band electrons, M is the magnetization per unit volume, g_{Mn} is the Landé g factor of the Mn^{2+} spins $=2$, and μ_B is the Bohr magneton.[16] The transitions in Fig. 2 labeled a and b occur for $\hat{\sigma}_+$ polarization, whereas those labeled c and d occur for $\hat{\sigma}_-$ polarization. The energies of the associated exciton transitions are

$$\begin{aligned} E_a&=E_0+3B-3A ,\\ E_b&=E_0+B+3A ,\\ E_c&=E_0-B-3A ,\\ E_d&=E_0-3B+3A , \end{aligned} \tag{7}$$

where E_0 differs from E_g by the exciton binding energy. These are the transitions observed in the Faraday geometry and are hence relevant for Faraday rotation. It has been shown that the a and d transitions are 3 times more probable than the b and c transitions.[16] Furthermore, with the magnitudes and signs of A and B in ZMT and CMT, the b and c transitions occur close to the zero-field transition, whereas a and d are shifted significantly below and above E_0.[17] In Table I we give recent determinations of $N_0\alpha$ and $N_0\beta$ for ZMT and CMT, where N_0 is the number of unit cells per unit volume. Thus it is clear that in the Faraday effect a and d will play a predominant role. Hence, to a good approximation, for ΔE_{ij} in Eq. (4) we may use

$$\Delta E_0=E_a(\hat{\sigma}_+)-E_d(\hat{\sigma}_-)=\frac{\beta-\alpha}{g_{\mathrm{Mn}}\mu_B}M , \tag{8}$$

and thus

$$\begin{aligned}\Theta_F&=E\frac{l}{2\hbar c}\frac{\partial n}{\partial E}\frac{\beta-\alpha}{g_{\mathrm{Mn}}\mu_B}M\\ &=\left[\frac{\sqrt{F_0}l}{2\hbar c}\frac{\beta-\alpha}{g_{\mathrm{Mn}}\mu_B}M\right]\frac{1}{E_0}\frac{y^2}{(1-y^2)^{3/2}} ,\end{aligned} \tag{9}$$

which expresses Θ_F explicitly in terms of the magnetization of the material. The parameter D, defined in Eq. (6b), is then

$$D=\frac{\sqrt{F_0}}{2\hbar c}\frac{\beta-\alpha}{g_{\mathrm{Mn}}\mu_B}\frac{\partial M}{\partial H} . \tag{10}$$

Further discussion about the form of the magnetization in DMS alloys as a function of x and T is given in the Appendix.

IV. EXPERIMENTAL RESULTS AND DISCUSSION

We will discuss our results for Faraday rotation in CMT and ZMT in three magnetic regimes: (A) low x at all temperatures, (B) arbitrary x at high temperatures, and (C) large x at low temperatures, where magnetic ordering occurs. We note that in cases (A) and (B) the alloy is paramagnetic.

TABLE I. Exchange energies for $Cd_{1-x}Mn_xTe$ and $Zn_{1-x}Mn_xTe$.

Crystal	$N_0\alpha$ (eV)	$N_0\beta$ (eV)
$Cd_{1-x}Mn_xTe$[a]	0.22	−0.88
$Zn_{1-x}Mn_xTe$[b]	0.19	−1.09

[a]Reference 19.
[b]Reference 17.

A. Faraday rotation versus temperature: Low-concentration regime

Figure 3(a) shows the dispersion of the Verdet constant for ZMT with $x=0.003$ for a series of temperatures. We note that at 300 K the Verdet constant is positive and its dispersion is nearly identical with that for ZnTe. As the temperature is lowered the effects of the *sp-d* exchange interaction overwhelm the intrinsic g factors of the valence and conduction bands and the Verdet constant becomes large and negative. It is clear from Fig. 3(a) that a positive Verdet constant persists at low photon energies. This background rotation may be due to contributions to the Faraday rotation arising from transitions between bands other than the valence and conduction bands.

The magnitude of the rotation seen at low temperatures is consistent with the increase in magnetization as the Mn^{2+} spins align more completely in a magnetic field. As shown in Eq. (9), the sign of the rotation is given by the sign of $\beta-\alpha$. Twardowski *et al.* have found from magnetization measurements and magnetotransmission studies of free excitons in ZMT that $N_0(\beta-\alpha)=-1.28$ eV.[17] Hence the expected sign of the Faraday rotation is negative. As shown in the Appendix, the magnetization for a very dilute system of Mn^{2+} spins is, to a good approximation, given by

$$M=-g_{\mathrm{Mn}}\mu_B x N_0\langle S_z^{\mathrm{Mn}}\rangle \text{ and } \langle S_z^{\mathrm{Mn}}\rangle=-\tfrac{5}{2}B_{5/2}(\eta)\ , \tag{11}$$

where $\langle S_z^{\mathrm{Mn}}\rangle$ is the thermal average of the Mn^{2+} spins along the direction of the applied magnetic field, $\eta=g_{\mathrm{Mn}}\mu_B H/k_B T$, k_B the Boltzmann constant, and $B_{5/2}$ is the Brillouin function B_J for $J=\frac{5}{2}$.[18] At low temperatures the effect of the *sp-d* exchange interaction will be large and can overshadow the intrinsic spin splitting of the energy bands, even for very low x.

For large H/T the effect of the *sp-d* exchange interaction will saturate, signaling the complete alignment of the Mn^{2+} spins along the applied magnetic field. This effect is clearly seen in Fig. 3(b), where we show the rotation for $\hbar\omega=2.29$ eV and $T=5$ K displayed as a function of magnetic field. The rotation shows observable saturation effects, expected from the Brillouin-function-like behavior of the magnetization. Following Eqs. (9) and (11), the dashed curve in Fig. 3(b) is a least-squares fit to the form $\Theta_F=\Theta_{\mathrm{sat}}B_{5/2}(\eta)$, where Θ_{sat} is a proportionality constant equal to $-671°$ and $T=4.2$ K. As can be seen, the Brillouin function fits the data very well and yields an acceptable sample temperature.

Similar results were obtained in CMT for $x=0.002$, as shown in Figs. 4(a) and 4(b). Note that $N_0(\beta-\alpha)$ in CMT is -1.10 eV[19] and hence V becomes negative at sufficiently low temperatures. The data in Fig. 4(b) are also well represented by a least-squares fit, with $\Theta_{\mathrm{sat}}=-1227°$ and $T=4.5$ K.

B. Faraday rotation in the high-temperature regime

The effects of increasing manganese concentration can be seen in Fig. 5. The figure displays Verdet dispersion curves at 300 K for ZMT with magnanese concentrations up to $x=0.10$. The Verdet dispersion bends down with increasing energy, and eventually reverses sign, the reversal taking place at lower and lower photon energies as more and more manganese is introduced. Qualitatively, with increasing manganese concentration, the DMS becomes progressively more paramagnetic, eventually overcoming the diamagnetic contribution to Faraday rotation characteristic of nonmagnetic II-VI compound semiconductors. In Fig. 6 we have a similar set of Verdet dispersion curves for CMT, observed at $T=300$ K for x ranging from 0 to 0.05. We see that the reversal of the sign of the Verdet constant observed in the ZMT also occurs in CMT.

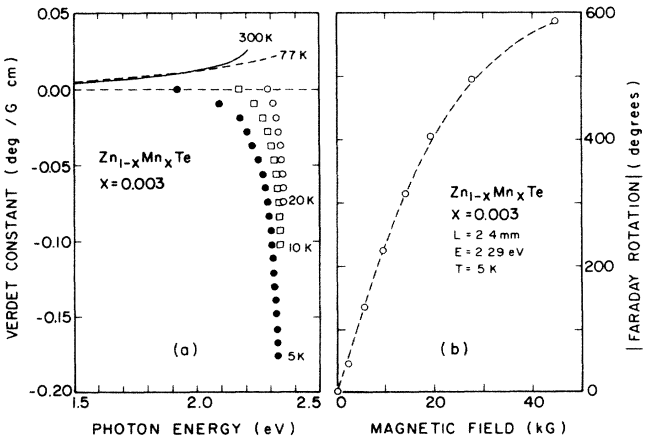

FIG. 3. (a) Verdet constant dispersion in $Zn_{1-x}Mn_xTe$, $x=0.003$, for a series of temperatures. (b) Magnetic field dependence of the Faraday rotation measured at 2.29 eV. The dashed line represents a least-squares fit of the form $\Theta_F=\Theta_{\mathrm{sat}}B_{5/2}(\eta)$, with $\Theta_{\mathrm{sat}}=-671°$ and $T=4.2$ K.

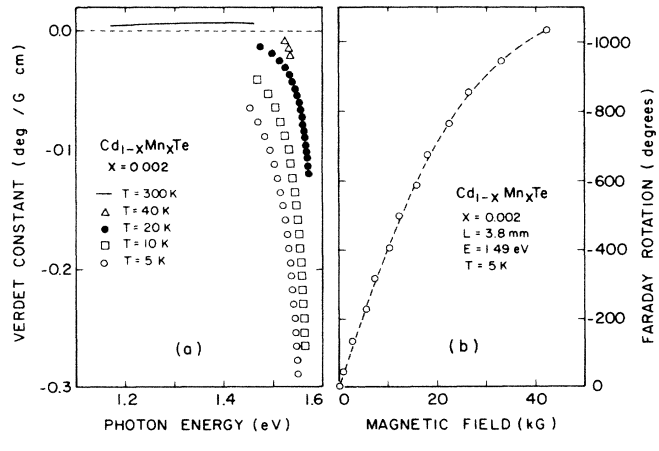

FIG. 4. (a) Verdet constant dispersion in $Cd_{1-x}Mn_xTe$, $x=0.002$, for a series of temperatures. (b) Magnetic field dependence of the Faraday rotation with increasing magnetic field showing saturation effects. The dashed line represents a least-squares fit of the form $\Theta_F=\Theta_{\mathrm{sat}}B_{5/2}(\eta)$, with $\Theta_{\mathrm{sat}}B_{5/2}=-1227°$ and $T=4.5$ K.

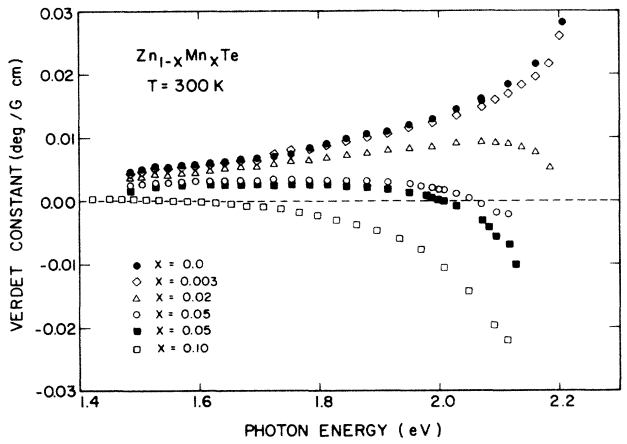

FIG. 5. Verdet dispersion for $Zn_{1-x}Mn_xTe$ at room temperature for several low values of x. The two sets of data for $x=0.05$ are for samples from different crystal boules that had the same nominal value of x.

As the manganese concentration is further increased beyond $x\simeq 0.20$ in ZMT, the sign of the Verdet constant at room temperature becomes negative over the entire photon-energy range investigated (1.20–2.10 eV). For the sample thickness used, the absorption at 2.1 eV associated with the internal levels of Mn^{2+} in DMS's (Ref. 15 and 20) prevented measurements beyond that energy. The Verdet dispersion in samples where the *sp-d* exchange interaction dominates over the entire spectral range ($x \geq 0.20$), when fitted to a single-oscillator model [Eq. (6b)], yields the parameters in Table II. The value for E_0 thus obtained agrees well with the energy of the free exciton for each sample.[20] This appears to support the single oscillator model.

We note that the internal transitions of Mn^{2+}, taking place near 2.1 eV, do not play an observable role in the Faraday effect. This observation is consistent with the fact that the transitions within the crystal-field-split internal levels of Mn^{2+} are not expected to contribute to Faraday rotation.[21,22] This observation is further corroborated by the data of Skowroński *et al.*, who measured the Verdet dispersion in ZMT with $x=0.10$ and $T=77$ K for photon energies well above the Mn^{2+} absorptions without observing any deviation from the single-oscillator behavior.[5]

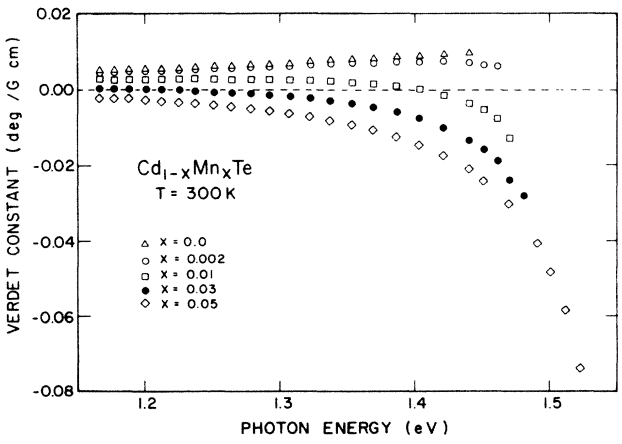

FIG. 6. Verdet dispersion curves for $Cd_{1-x}Mn_xTe$ at room temperature for several low values of x.

We also note that in the high-temperature regime the magnetization varies linearly with H and the magnetic susceptibility has a Curie-Weiss form, as described in the Appendix. Using this form for M in Eq. (10), we can write the single-oscillator parameter D as

$$D=\frac{35}{12}\frac{\sqrt{F_0}}{2\hbar c}\frac{g_{\mathrm{Mn}}\mu_B N_0(\beta-\alpha)x}{k_B(T+\Theta_0 x)}\ , \tag{12}$$

where Θ_0 is -470 and -831 K for CMT and ZMT, respectively. Thus, the Faraday effect would prove to be a useful tool for studying DMS's in this regime, particularly in determining Θ_0.

As we have noted, both ZMT and CMT exhibit a small, positive rotation at low photon energies [see Figs. 3(a), 4(a), 5, and 6]. This positive rotation is compensated for by the negative contribution arising from the influence of the *sp-d* exchange interaction on the free exciton, as is evident for increasing x or for increasing photon energies at a given value of x. In the single-oscillator (exciton) model, in which the oscillator undergoes a Zeeman splitting completely governed by the *sp-d* exchange interaction, the Faraday rotation will have the same sign over the entire spectral range, as can be seen from Eq. (9). The background, positive rotation thus appears to be connected with additional electronic transitions which are influenced by Mn^{2+} in a different manner than the Γ_8 valence band and the Γ_6 conduction band; for example, transitions from deep and split-off valence bands to conduction bands, none of which are affected in the same manner by the exchange interaction, may be responsible for this positive "background" rotation.

C. Faraday rotation in the magnetically ordered regime

As was first demonstrated by Galazka, Nagata, and Keesom,[3] a magnetic phase transition to the spin-glass occurs in DMS crystals when x exceeds, and temperature is below, a critical value. Motivated by this, we have extended our studies of the Faraday rotation in CMT to higher values of x and lower temperatures.

As pointed out in the Appendix, in the regime of high x and low T the magnetization can no longer be formulat-

TABLE II. Exciton and single-oscillator model parameters for $Zn_{1-x}Mn_xTe$ at room temperature [see Eq. (6b)].

	Expt.	Fitting parameters	
x	E^{a}_{exciton} (eV)	E_0 (eV)	D (10^{-3}deg eV/G cm)
0.24	2.40	2.38	−17.6
0.34	2.45	2.46	−22.9
0.51	2.54	2.57	−33.7
0.69	2.63	2.65	−39.0

[a]Reference 20.

ed analytically, but may be roughly approximated by a modified Brillouin function

$$M=\bar{x}N_0 g_{\mathrm{Mn}}\mu_B \times \tfrac{5}{2}B_{5/2}(\eta')\ , \tag{13}$$

where

$$\eta'=\frac{g_{\mathrm{Mn}}\mu_B H}{k_B(T+T_{\mathrm{AF}})}\ .$$

In the limit of low magnetic fields $B_{5/2}(\eta')=\frac{7}{6}\eta'$, and by substituting this into Eqs. (12) and (10) we may write the single-oscillator parameter D as

$$D=\frac{35}{12}\frac{\sqrt{F_0}}{2\hbar c}\frac{g_{\mathrm{Mn}}\mu_B N_0(\beta-\alpha)\bar{x}}{k_B(T+T_{\mathrm{AF}})}\ . \tag{14}$$

The Faraday rotation for a series of CMT samples and one ZMT sample was measured over a wide temperature range. The sign of the rotation was negative over the entire spectral range investigated, and the dispersion of the rotation was well described by the single-oscillator model. Fitting our results to this model, Eq. (6b), we obtain D for each sample. Figure 7 shows a plot of D^{-1} versus T for some of the CMT samples. It is found that for $T\leq 40$ K the data for $x=0.05$, 0.10, 0.23, and 0.35 can be fitted with

$$D^{-1}=m(T+T_{\mathrm{AF}})\ ,$$

where m is the slope of the least-squares fits (AF denotes antiferromagnetic). These results are summarized in Table III.

Some general trends are apparent from Table III. For increasing x, m decreases as expected from Eq. (14) although the decrease is not linear with x. This is most likely an indication that the ratio $\bar{x}/x$ decreases with increasing x due to magnetic coupling between Mn^{2+} ions. We also note that T_{AF} increases with increasing x. For $x=0.05$, the straight-line fit displayed in Fig. 7 nearly intercepts the temperature axis at $T=0$, as would be expected if the Mn^{2+} ions were independent of one another. The nonzero value of $T_{\mathrm{AF}}=1.0$ K indicates that the

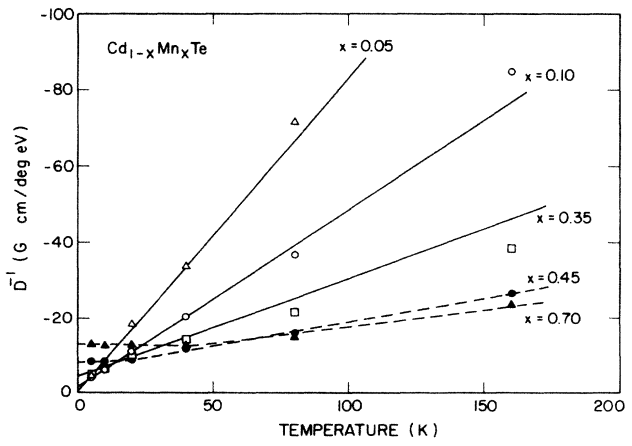

FIG. 7. D^{-1} versus temperature for some of the $Cd_{1-x}Mn_xTe$ samples studied. The straight lines are least-squares fits to the data points for $T\leq 40$ K. The dashed curves for $x=0.45$ and 0.70 are drawn as a visual aid. See Table III for parameters.

TABLE III. Linear least-squares-fit parameters for D^{-1} vs T ($T\leq 40$ K).

x	m (G cm/deg eV K)	T_{AF} (K)	T^{a}_{AF} (K)	x^{a}
0.05	−0.829	1.0	2.25	0.05
0.10	−0.468	3.3	3.37	0.10
0.23	−0.352	7.3	6.24	0.25
0.35	−0.261	15.2	16.2	0.30

[a]Reference 23.

Mn^{2+} ions are indeed experiencing some magnetic coupling. For higher x the magnetic coupling becomes more noticeable, as evidenced by the increasing T_{AF}. One may compare these values of T_{AF} to those determined from donor spin-flip Raman scattering measurements,[23] also displayed in Table III; the agreement is qualitatively good.

The data for $x=0.45$ show a marked deviation from linear behavior, as can be seen in Fig. 7. The curve levels off for temperatures less than about 20 K. At $T\simeq 15$ K there is a paramagnetic—to—spin-glass phase transition. It seems reasonable to speculate that the leveling off is a manifestation of the spin-glass phase. The data for $x=0.70$, in fact, show a slight increase in $|D^{-1}|$ with decreasing temperatures below 40 K. We note that magnetic ordering in $Cd_{0.3}Mn_{0.7}Te$ indeed occurs near 40 K.[24] In ZMT a similar trend is observed for $x=0.69$. Thus Faraday rotation is clearly sensitive to the magnetic phase transitions of DMS's.

At this point we draw attention to work done by Mycielski *et al.*[25] in $Hg_{1-x}Mn_xTe$ and Kierzek-Pecold *et al.*[26] in $Cd_{1-x}Mn_xTe$, where Faraday rotation is used as a tool to study the spin-glass phase transition. In both of these measurements the Faraday rotation was monitored at a fixed field as the temperature was changed. The above authors observe *kinks* in the rotation at the expected temperatures for the spin-glass transition.

V. CONCLUSIONS

In the present investigation the dispersion of the interband Faraday effect in $Zn_{1-x}Mn_xTe$ and $Cd_{1-x}Mn_xTe$ has been studied over a wide range of Mn concentrations and temperatures. Using samples with very small values of x, the increasing contribution to the rotation due to the effects of the *sp-d* exchange interaction and its eventual dominance over the intrinsic g factors of the valence and conduction bands is demonstrated. The rotation tends to saturate at high magnetic fields, corresponding to complete alignment of the Mn^{2+} spins. For low x and high T the rotation is small and positive at low photon energies, but becomes large and negative for photon energies close to that of the free exciton. At room temperature, as x increases, the sign of the Verdet dispersion becomes negative, signaling the departure of the DMS from the diamagnetic regime into the paramagnetic regime. When the diamagnetic contribution is overwhelmed by the *sp-d* exchange interaction, the dispersion of the Verdet constant can be described by a single-oscillator model with the transition energy corresponding to that of the free exciton. As the temperature is decreased we see the effects

of the antiferromagnetic coupling between the Mn^{2+} spins acting to reduce the magnitude of the rotation, the effect becoming more pronounced with increasing x. Finally, we observed no effect on the rotation due to the Mn^{2+} absorption band located at ~ 2.1 eV.

Two questions appear to emerge from the above study.

(1) Although we have labeled the rotation in ZMT and CMT as excitonic rotation, it is not clear why this model should work so well. Interband models such as those developed by Boswarva *et al.*[12] and Roth[13] explain the Verdet dispersion of nonmagnetic II-VI compound crystals very well. Excitonic effects have been seen in the Faraday effect in CdTe,[27] but only for photon energies very close to the energy gap. For DMS alloys, the excitonic Faraday effect appears to dominate over the entire spectral range.

(2) In general, the entire energy band structure will contribute to the Faraday effect. A better understanding of the *sp-d* exchange interaction for electronic transitions away from the Brillouin-zone center, as well as for spin-orbit-split bands, has yet to be developed.

ACKNOWLEDGMENTS

The authors thank S. Rodriguez, D. L. Peterson, M. Dutta, and A. Petrou for their valuable comments and discussions during the course of this work, as well as U. Debska, R. R. Galazka, and W. Giriat for the samples used in this work. This research was supported by the U. S. Office of Naval Research under Contract No. N00014-82-K0563. Part of the measurements were carried out using the Purdue University Laser Facility supported by the National Science Foundation (NSF) Materials Research Laboratory Program (MRL) under Grant No. DMR-83-16988.

APPENDIX: MAGNETIZATION IN DMS ALLOYS

Faraday rotation is a function of frequency, of oscillator strengths corresponding to the dominant transitions, of exchange integrals, and of the magnetization M. It is the latter that gives it its dependence on manganese concentration and magnetic field. Since the dependence of M on these parameters is complicated, we find it useful to briefly review the magnetic behavior of DMS's in various parameter ranges. We discuss the magnetization M in three regimes, in which useful analytic forms of expressing M and Θ_F can be developed.

1. Low concentration of magnetic ions

In this regime M can be formulated from first principles. We can write

$$M = xN_0 g_{\mathrm{Mn}} \mu_B S B_S(\eta) , \tag{A1}$$

where $\eta = g_{\mathrm{Mn}} \mu_B H / k_B T$, x is the manganese concentration, and $S = \frac{5}{2}$ for Mn-based DMS's, other symbols being standard. Sometimes the above is written as

$$M = -g_{\mathrm{Mn}} \mu_B x N_0 \langle S_z^{\mathrm{Mn}} \rangle , \tag{A2}$$

where $\langle S_z^{\mathrm{Mn}} \rangle = -S B_S(\eta)$. For low values of the argument η, i.e., for low magnetic fields or high T, the Brillouin function can be expanded, $B_S(\eta) = [(S+1)/3]\eta$. Then

$$M = xN_0 (g_{\mathrm{Mn}} \mu_B)^2 \frac{S(S+1)}{3k_B T} H , \tag{A3}$$

$$\langle S_z^{\mathrm{Mn}} \rangle = -\frac{g_{\mathrm{Mn}} \mu_B S(S+1)}{3k_B T} H , \tag{A4}$$

$$\chi = xN_0 (g_{\mathrm{Mn}} \mu_B)^2 \frac{S(S+1)}{3k_B T} \equiv \frac{C(x)}{T} . \tag{A5}$$

Thus, for this region Θ_F can be written as

$$\Theta_F = \frac{\sqrt{F_0} l}{2\hbar c} x N_0 (\beta - \alpha) S B_S(\eta) \frac{\hbar^2 \omega^2}{(E_0^2 - \hbar^2 \omega^2)^{3/2}} , \tag{A6}$$

which at low η gives the linear (Verdet constant) region of Faraday rotation,

$$\Theta_F = \frac{\sqrt{F_0} l}{2\hbar c} x N_0 (\beta - \alpha)(g_{\mathrm{Mn}} \mu_B) \frac{S(S+1)}{3k_B T} H \frac{\hbar^2 \omega^2}{(E_0^2 - \hbar^2 \omega^2)^{3/2}} , \tag{A7}$$

where $\hbar\omega$ is the photon energy and E_0 the oscillator transition energy.

2. High-temperature limit (arbitrary x)

At high temperatures DMS's of arbitrary x can be analytically discussed in the low-field region (i.e., where M is linear in H). The magnetic susceptibility $\chi (= M/H)$ then displays the Curie-Weiss behavior

$$\chi = \frac{C(x)}{T - \Theta(x)} = \frac{C_0 x}{T + \Theta_0 x} , \tag{A8}$$

where

$$C(x) = \frac{x N_0 (g_{\mathrm{Mn}} \mu_B)^2 S(S+1)}{3k_B} ,$$

and Θ_0 can be described analytically for nearest-neighbor interactions,

$$\Theta_0 = -\frac{8S(S+1) J_{\mathrm{NN}}}{k_B} \tag{A9}$$

[see Eqs. (2.14) and (5.2) in Spałek *et al.*[28]] Here, J_{NN} is the nearest-neighbor exchange integral.

The parameter Θ_0 varies from material (i.e., II-VI compound parent) to material, ranging from 400 to 900 K. Note that this can be used to define limits on x where the Curie behavior applies. Typically, when $\Theta_0 x \ll T$, we can use the results from the preceding section (at least for χ).

In this parameter range Θ_F can be formulated analytically for the region where M varies linearly with H. It then becomes

$$\Theta_F = \frac{\sqrt{F_0} l}{2\hbar c} \frac{\beta - \alpha}{g_{\mathrm{Mn}} \mu_B} \frac{C_0 x}{T + \Theta_0 x} H \frac{\hbar^2 \omega^2}{(E_0^2 - \hbar^2 \omega^2)^{3/2}} , \tag{A10}$$

where Θ_0 is 470 and 831 K for CMT and ZMT, respectively.[28]

3. The low-temperature, high-x region

For higher x, magnetization M has not been analytically formulated. By "higher x" we mean any x which is sufficient to form a significant population of Mn^{2+} pairs and higher complexes (triplets, etc.) The reason for this is that with Mn^{2+} complexes present the saturation of the magnetization with magnetic field will contain a series of steps corresponding to the dissociation of pairs, triplets, etc.[29] It is only in the highest fields (perhaps MG) that the Brillouin function will rigorously apply. Thus, if our vision is limited to below the first magnetization step, we would get erroneous parameters by assuming that what we see (below the step) is described by the Brillouin function.

Thus, if we have $x > 0.05$, where there are already many Mn^{2+} complexes, we would see saturation effects, but these are not described by the Brillouin function. Probably when looking at the magnetization versus field we would see a curve composed of unresolved steps. Noting the similarity of this behavior to the Brillouin function, Gaj *et al.*[19] proposed that M can be expressed by an *effective* Brillouin function in which one replaces T by an effective temperature T_{eff}.[16] T_{eff} can be written as

$$T_{\text{eff}} = T + T_{\text{AF}} , \tag{A11}$$

in the spirit of the Curie-Weiss formula. The analogy of T_{AF} with the Curie-Weiss temperature Θ_{CW} as usually defined (see preceding section) is somewhat unfortunate in that it suggests that at high temperature T_{AF} will merge with Θ_{CW}, which is not the case.

T_{AF} (and thus T_{eff}) is merely an empirical coefficient, which is a function of x *and* T, and which gives the *profile* of M versus H for a given x and T. It is found, furthermore, that to give the correct *magnitude* of M, in the equation for M we must replace x by an *effective* manganese concentration $\bar{x}$, i.e.,

$$M = \bar{x} N_0 g_{\text{Mn}} \mu_B S B_S \left[\frac{g_{\text{Mn}} \mu_B H}{k_B T_{\text{eff}}} \right] . \tag{A12}$$

The above formulation does not have theoretical foundations, but is simply a convenient way in which to express M in terms of two phenomenological quantities that must be established for each concentration and temperature.

It is clear from the above discussion that the Faraday effect can be used to observe magnetically coupled Mn^{2+} pairs, triplets, etc. The effects associated with Mn^{2+} complexes should appear as steps in the Faraday rotation as the magnetic field is increased and these complexes dissociate.

[1] J. K. Furdyna, J. Appl. Phys. **53**, 7637 (1982).

[2] A. K. Ramdas, J. Appl. Phys. **53**, 7649 (1982).

[3] R. R. Galazka, Shoichi Nagata, and P. H. Keesom, Phys. Rev. B **22**, 3344 (1980). See also S. B. Oseroff, *ibid.* **25**, 6584 (1982).

[4] J. A. Gaj, R. R. Galzka, and M. Nawrocki, Solid State Commun. **25**, 193 (1978).

[5] M. Skowroński, J. M. Baranowski, and L. J. Ludwicki, in *Materiały VIII Ogólnokrajowego Seminarium Zwiazków* Półprzewodnikowych, Jaszowiec, Jaszowiec, 1977 (Prace Instytutu Fizyki, Polska Akademia Nauk **75**, Warszawa, 1978), p. 127.

[6] A. Ebina, T. Koda, and S. Shionoya J. Phys. Chem. Solids **26**, 1497 (1965).

[7] *V*-4005 4-in. electromagnet. Varian Associates, Palo Alto, CA 94303. Measurements were made with 2-in. tapered pole pieces for magnetic fields up to 21 kG with a gap spacing of 0.5 in.

[8] V. Prosser, Czech. J. Phys. B **15**, 128 (1965).

[9] Model 10 DT "Super-Varitemp" Optical Magnetic Cryostat, Janis Research Co., Wilmington, MA 01887; the superconducting coil was manufactured by American Magnetics, Inc., Oak Ridge, TN 37830.

[10] Model 14018, Spex Industries, Inc. Metuchen, NJ 08840.

[11] C. R. Pidgeon and S. D. Smith, Infrared Phys. **4**, 13 (1964).

[12] I. M. Boswarva, R. E. Howard, and A. B. Lidiard, Proc. R. Soc. London, Ser. A **269**, 125 (1962).

[13] L. M. Roth, Phys. Rev. **133**, A **542**, (1964).

[14] M. Balkanski, E. Amzallag, and D. Langer, J. Phys. Chem. Solids **27**, 299 (1966).

[15] Y. R. Lee, A. K. Ramdas, and R. L. Aggarwal, Phys. Rev. B **33**, 7383 (1986).

[16] J. A. Gaj, J. Ginter, and R. Galazka, Phys. Status Solidi B **89**, 655 (1978).

[17] A. Twardowski, P. Swiderski, M. von Ortenberg, and R. Pauthenet, Solid State Commun. **50**, 509 (1984).

[18] F. Reif, *Fundamentals of Statistical and Thermal Physics* (McGraw-Hill, New York, 1965), p. 259.

[19] J. A. Gaj, R. Planel, and G. Fishman, Solid State Commun. **29**, 435 (1979).

[20] Y. R. Lee and A. K. Ramdas, Solid State Commun. **51**, 861 (1984); Bull Am. Phys. Soc. **30**, 214 (1985).

[21] C. J. Ballhausen, *Introduction to Ligand Field Theory* (McGraw-Hill, New York, 1962), Chap. 9.

[22] Y. R. Shen, Phys. Rev. **133**, A511 (1964).

[23] D. L. Peterson, D. U. Bartholomew, U. Debska, A. K. Ramdas, and S. Rodriguez, Phys. Rev. B **32**, 323 (1985).

[24] S. Venugopalan, A. Petrou, R. R. Galazka, A. K. Ramdas, and S. Rodriguez, Phys. Rev. B **25**, 2681 (1982).

[25] A. Mycielski, C. Rigaux, and M. Menant, Solid State Commun. **50**, 257 (1984).

[26] E. Kierzek-Pecold, W. Szymańska, and R. R. Galazka, Solid State Commun. **50**, 685 (1984).

[27] P. S. Kireev, L. V. Volova, and V. V. Volkov, Fiz. Tekh. Poloprovdn. **5**, 2080 (1971) [Sov. Phys.—Semicond. **5**, 1812 (1972)].

[28] J. Spałek, A. Lewicki, Z. Tarnawski, J. K. Furdyna, R. R. Galazka, and Z. Obuszko, Phys. Rev. B **33**, 3407 (1986).

[29] Y. Shapira, S. Foner, D. H. Ridgley, K. Dwight, and A. Wold, Phys. Rev. B **30**, 4021 (1984); R. L. Aggarwal, S. N. Jasperson, P. Becla, and R. R. Galazka, *ibid.* **32**, 5132 (1985).

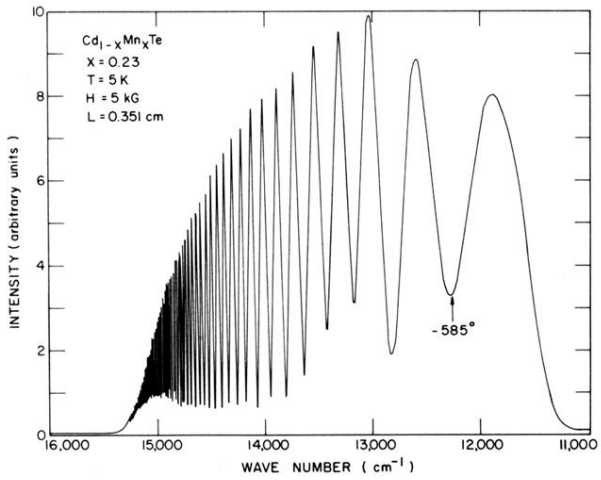

FIG. 1. Transmission spectrum through $Cd_{1-x}Mn_xTe$, $x=0.23$, in the Faraday geometry at $T=5$ K and $H=5$ kG displaying giant Faraday rotations several orders of magnitude larger than those seen in CdTe. The intensity cutoff at low photon energies is due to the photomultiplier-tube response, whereas the cutoff at high energies is due to the absorption edge of the sample. The minima of the transmission oscillations are not zero as a result of increasing Faraday ellipticity near the absorption edge.